Theor Chem Account (2009) 122:189–196
DOI 10.1007/s00214-008-0498-4

REGULAR ARTICLE

A theoretical study on photodissociation of the *A* state of the H_2S^+ ion

Hai-Bo Chang · Ming-Bao Huang

Received: 19 September 2008 / Accepted: 2 December 2008 / Published online: 19 December 2008
© Springer-Verlag 2008

Abstract We have studied photodissociation of the A state of the H_2S^+ ion using the quantum-chemical CAS methods, and the $1^2A''$ (X^2B_1) and $1^4A''$ states are involved in photodissociation of the $1^2A'$ (A^2A_1) state (the electronic states in dissociation were studied in the C_s symmetry). The CASPT2 S-loss dissociation potential energy curve (PEC) calculations indicate that the $1^2A''$ and $1^2A'$ states correlate with the second limit [$H_2 + S^+(^2D)$] while the $1^4A''$ state correlates with the first limit [$H_2 + S^+(^4S)$] and that there are a transition state and a local minimum along the $1^2A'$ PEC and the repulsive $1^4A''$ PEC crosses the $1^2A''$ and $1^2A'$ PECs. The CASPT2 H-loss dissociation PEC calculations indicate that the $1^2A''$ and $1^4A''$ states correlate with the first limit [$HS^+(X^3\Sigma^-) + H$] while the $1^2A'$ state correlates with the second limit [$HS^+(a^1\Delta) + H$] and that the repulsive $1^4A''$ PEC crosses the $1^2A'$ PEC. For the crossing doublet and quartet states in pairs, we performed CASSCF minimum energy crossing point (MECP) calculations, and the CASSCF spin-orbit couplings and CASPT2 energies at the MECP geometries were calculated. We examined the two previously proposed mechanisms (mechanisms I and II) for dissociation of the *A* state to the S^+ ion, based on our calculation results. We suggest processes for dissociation of the *A* state to the S^+ ion (processes I and II, based on mechanisms I and II, respectively) and to the SH^+ ion (process III) and conclude that photodissociation of the *A* state mainly leads to the S^+ ion via the most energetically favorable process II: A^2A_1 ($1^2A'$) (2.38 eV) → barrier at the linearity (2.96 eV) → X^2B_1 ($1^2A''$) (0.0 eV) → the $1^2A''/1^4A''$ MECP (3.50 eV, large spin-orbit coupling) → $H_2(X^1\Sigma_g^+) + S^+(^4S)$ (2.92 eV) (the CASPT2 relative energy values to X^2B_1 are given in parentheses and the largest value is 3.50 eV at the MECP).

Keywords H_2S^+ ion · CASPT2 · Photodissociation

1 Introduction

Theoretical studies [1–3] on low-lying electronic states of the H_2S^+ ion were difficult because in the C_{2v} symmetry the *B* state should be assigned to 1^2B_2 while the calculated adiabatic excitation energy (T_0) values for 1^2B_2 were about 1 eV smaller than the experimental value for the *B* state. The difficulty could be removed [3] when the low-lying states of H_2S^+ were studied within the C_s symmetry: the *X*, *A*, and *B* states were assigned to $1^2A''$, $1^2A'$, and $2^2A'$, respectively, and the calculated T_0 values for the $1^2A'$ and $2^2A'$ states were in reasonable agreement with the experimental T_0 values for the *A* and *B* states, respectively [3]. In the present study we focus on photodissociation of the *A* state of the H_2S^+ ion.

During the past several decades, numerous experimental studies [4–20] and some theoretical studies [1, 2] on S-loss and H-loss dissociation from excited electronic states of the H_2S^+ ion were reported. The experimental workers always paid attention to the product S^+ and SH^+ ions. On the basis of his experiments [8] Eland concluded that the product S^+ ion in the dissociation of the H_2S^+ ion be mainly attributed to the dissociation of the *A* state, and his conclusion was supported by the experiments of Prest et al. [12]. There were two proposed mechanisms for the dissociation of the

H.-B. Chang · M.-B. Huang (✉)
College of Chemistry and Chemical Engineering,
Graduate University of Chinese Academy of Sciences,
P. O. Box 4588, Beijing 100049,
People's Republic of China
e-mail: mbhuang1@gucas.ac.cn

A state to the S^+ ion. On the basis of their MRD-CI calculation results Hirsch et al. [2] proposed the following mechanism (denoted as mechanism I in the present article, see Scheme 1): the A^2A_1 state nonadiabatically transits to the B^2B_2 state via strong vibronic coupling followed by another transition to the 1^4A_2 state by spin-orbit coupling, finally producing $S^+(^4S) + H_2$. They calculated only the C_{2v} states and did not calculate the dissociation reaction paths. Dixon et al. [10] suggested an alternative dissociation mechanism (denoted as mechanism II in the present article, see Scheme 1) as follows: the A^2A_1 state nonadiabatically transits to the X^2B_1 state via the Renner–Teller coupling around the linear configuration followed by another transition to the 1^4A_2 state by spin–orbit coupling, finally producing $S^+(^4S) + H_2$.

Hirst [1] claimed that mechanism II was supported by his MRCI potential energy surface calculations for low-lying electronic states of the H_2S^+ ion and made no comments on mechanism I. His potential energy surfaces (PESs) were represented by the two-dimensional contour diagrams (with a third geometric parameter fixed at a certain value), which are actually some sections of the PESs. We note that Webb et al. [4] proposed that both of mechanisms I and II may be responsible for the products $[S^+(^4S) + H_2]$ within their experimental wavelength range.

In the present theoretical work we mainly study photodissociation from the A state of the H_2S^+ ion using the complete active space self-consistent-field (CASSCF) [21] and multiconfiguration second-order perturbation theory (CASPT2) [22, 23] methods. These methods are considered to be effective for theoretical studies on excited electronic states and photodissociation of molecular ions [24]. By performing the CASPT2 potential energy curve (PEC) calculations for adiabatic S- and H-dissociation from the A and other (X and $1^4A''$) states and the CASSCF calculations for minimum energy crossing points (MECPs) between the doublet and quartet states, we examine the previously proposed mechanisms I and II for dissociation of the A state to the S^+ ion. Based on our calculation results we will suggest processes for dissociation of the A state to the S^+ ion and to the HS^+ ion and determine the most energetically favorable process.

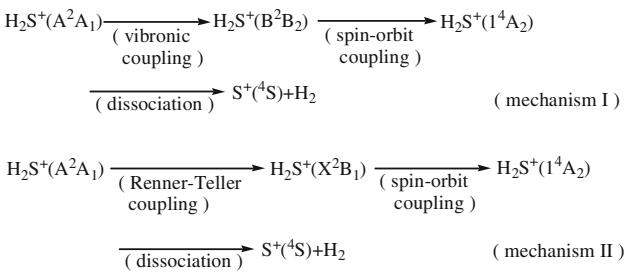

Scheme 1 Previously proposed mechanisms

2 Calculation details

Geometry and atom labelings used for the H_2S^+ ionic system (C_s) used in the present work are shown in Fig. 1 (M denotes the mid-point of the H_1–H_2 bond distance). As we mentioned above, we previously studied electronic states of the H_2S^+ ion in the C_s symmetry [3]. In the present work we have studied dissociation of electronic states of the H_2S^+ ionic system also in the C_s symmetry. In the theoretical study on photodissociation of the A state, we have focused our attention on the $1^2A''$ (X^2B_1), $1^2A'$ (A^2A_1), and $1^4A''$ states of the H_2S^+ ionic system (see Sect. 3), though we also calculated H-loss dissociation PEC for the $2^2A'$ (B) state.

The CASSCF and CASPT2 calculations were carried out using the MOLCAS v 6.2 quantum-chemistry software [25]. With a CASSCF wave function constituting the reference function, the CASPT2 calculations were performed to compute the first-order wavefunction and the second-order energy in the full-space. A contracted atomic natural orbital (ANO) basis set, [26–28] S[6s4p3d1f]/H[3s2p1d], was used.

In our CAS calculations for electronic states of the H_2S^+ ionic system, 11 electrons were active and the active space included 12 orbitals [denoted as CAS (11, 12)]. The choice of the active space stemmed from the electron configuration (based on the HF/6-3lG(d) calculations) of the ground-state H_2S molecule: $[\ldots(3a_1)^2(1b_1)^2(4a_1)^2(2b_2)^2(5a_1)^2(2b_1)^2(3b_2)^0(6a_1)^0(7a_1)^0(4b_2)^0(8a_1)^0(3b_1)^0\ldots]$, Within the C_s point group, the electron configuration is $[\ldots(4a')^2(1a'')^2(5a')^2(6a')^2(7a')^2(2a'')^2(8a')^0(9a')^0(10a')^0(11a')^0(12a')^0(3a'')^0\ldots]$, and all the 12 orbitals (six occupied plus six virtual) listed in the square bracket were taken as active orbitals. We also performed CASPT2 calculations for possible dissociation products. In the CAS calculations for low-lying electronic states of the S^+ ion, 13 electrons were active and the active space included 2s, 2p, 3s, and 3p orbitals. In the CAS calculations for the ground-state H_2 molecule, two electrons were active and the active space included two orbitals. In the CAS calculations for the three lowest-lying states of the HS^+ ion, 14 electrons were active, and the active space included nine orbitals

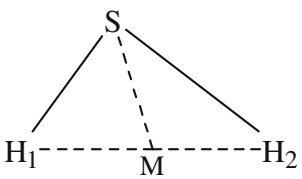

Fig. 1 Atom labelings for the H_2S^+ ion (C_s) used in the present work (M denotes the mid-point of the H_1–H_2 bond distance)

involving the 2s, 2p, 3s, and 3p orbitals of the S atom and the 1s orbital of the H atom. The space used for H_2S^+ was too large since we had wanted to calculate many ionic states at the very beginning. However, the CASPT2 calculation results are not too sensitive to the size of active spaces if they are already large. In the CASPT2 calculations, the weight values of the CASSCF reference functions in the first-order wave functions were larger than 0.95.

In the present study we performed CASPT2 calculations for the $1^2A''(X)$ and $1^2A'(A)$ states of the H_2S^+ ion using the active space mentioned above. The present calculations produced almost the same geometric and energetic results as those reported in Ref. [3]. The CASPT2 optimized geometries for the $1^2A''$ and $1^2A'$ states and the CASPT2 T_0 value (2.38 eV) for $1^2A'$ are listed in Table 1.

3 Results and discussion

3.1 CASPT2 S-loss dissociation potential energy curves for the low-lying states

We calculated S-loss dissociation PECs for the $1^2A''$ (X^2B_1) and $1^2A'$ (A^2A_1) states of the H_2S^+ ion. We also calculated the PEC of the $1^4A''$ (1^4A_2) state. As we will see below, this state correlates with the first limit of the *S*-loss dissociation and its PEC crosses the $1^2A''$ and $1^2A'$ PECs.

The *S*-loss dissociation PECs for the three states were calculated at the CASPT2 level. At a set of fixed *R*(S–M) (Fig. 1) values ranging from the *R*(S–M) values in the CASPT2 optimized geometries of the respective states (from *R*(S–M) = 1.4 Å for $1^4A''$) to 4.0 Å, the CASPT2 partial geometry optimization calculations were performed for the three states. The S-loss dissociation PECs for the $1^2A''$, $1^2A'$, and $1^4A''$ states were drawn in Fig. 2 on the basis of the CASPT2 energies at the three sets of partially optimized geometries. The H_2S^+ systems in the three states

Table 1 CASPT2 calculation results for the $1^2A''$ and $1^2A'$ states of the H_2S^+ ion: the optimized geometries and relative energies [ΔE (T_0) in eV, to X^2B_1] for the minima in the two states and the transition state and local minimum in the $1^2A'$ state (bond lengths are in Å and bond angles in degrees)

State	Stationary point	R(S–H$_1$)	R(S–H$_2$)	∠HSH	ΔE	Exptl. T_0
$1^2A''$	Minimum (X^2B_1)	1.357	1.357	93.0	0.0	0.0
$1^2A'$	Minimum (A^2A_1)	1.356	1.356	126.6	2.38	2.31[a]
	Transition state ($1^2A'$)	1.382	1.563	71.8	4.06	
	Local minimum ($1^2A'$)	1.547	1.547	33.7	3.20	

[a] Ref. [34]

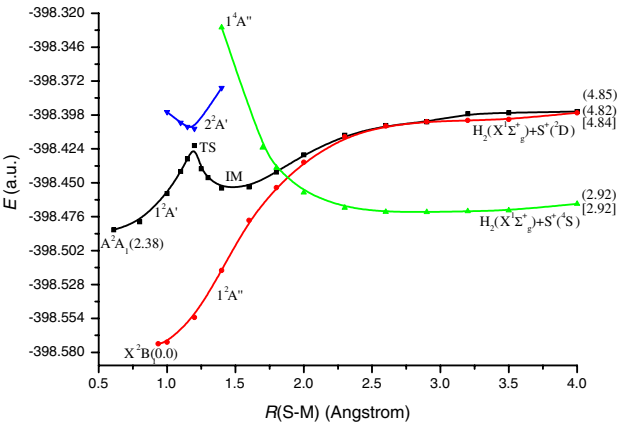

Fig. 2 CASPT2 potential energy curves (PECs) for S-loss dissociation from the $1^2A''$ (X^2B_1), $1^2A'$ (A^2A_1), and $1^4A''$ states of the H_2S^+ ion. The *values* in parentheses are the CASPT2 energies (relative to X^2B_1, in eV) of the reactants and asymptotic products and the values in square brackets are the CASPT2 energies (energy sums) (relative to X^2B_1, in eV) of the dissociation products

at the *R*(S–M) value of 4.0 Å will be called as S-loss dissociation asymptotic products of the respective states in the present article.

In the three asymptotic products the charge values at the S atom are close to the unity (>0.997e) and the distances between the two H atoms are all equal to 0.740 Å (the experimental bond length value for $H_2(X^1\Sigma_g^+)$ being 0.741 Å [29]), which indicates that the dissociation products for the three states are the ground-state H_2 molecule plus the S^+ ion in different states. The CASPT2 geometry optimization calculations (see Sect. 2) for the ground-state H_2 molecule and the CASPT2 energy calculations (see Sect. 2) for the ^4S_u ground and first excited ^2D_u states of the S^+ ion were performed. These CASPT2 calculations predict that the energy sum of $H_2(X^1\Sigma_g^+) + S^+(^4S)$ (the first limit for S-loss dissociation) is 2.92 eV above the X^2B_1 reactant and the energy sum of $H_2(X^1\Sigma_g^+) + S^+(^2D_u)$ (the second limit for S-loss dissociation) is 4.84 eV above X^2B_1. The CASPT2 energy value for the $1^4A''$ asymptotic product is identical to the CASPT2 energy sum of $H_2(X^1\Sigma_g^+) + S^+(^4S)$, which confirms that the S-loss dissociation products from the $1^4A''$ state of the H_2S^+ ion are $[H_2(X^1\Sigma_g^+) + S^+(^4S)]$ (the first limit for S-loss dissociation). The CASPT2 energy values for the $1^2A''$ and $1^2A'$ asymptotic products are close to the CASPT2 energy sum of $H_2(X^1\Sigma_g^+) + S^+(^2D_u)$ (the deviations being not larger than 0.02 eV), which confirms that the S-loss dissociation products from the $1^2A''$ (X^2B_1) and $1^2A'$ (A^2A_1) states of the H_2S^+ ion are $[H_2(X^1\Sigma_g^+) + S^+(^2D)]$ (the second limit for S-loss dissociation). The CASPT2 relative energies (to X^2B_1) of the reactants, asymptotic products, and products for the S-loss dissociation from the $1^2A''$ (X^2B_1), $1^2A'$ (A^2A_1), and $1^4A''$ states are given in Table 2.

Table 2 The critical points [reactants, minimum energy crossing points (MECP), transition states (TS), intermediates (IM), asymptotic products (AsP), and products] along the CASPT2 S-loss dissociation PECs of the $1^2A''$ (X^2B_1), $1^2A'$ (A^2A_1), and $1^4A''$ states of the H_2S^+ ion: locations [R(S–M) values in Å] and relative energies (ΔE in eV, to X^2B_1)

State	Reactant	TS	IM	MECP	AsP	Products
$1^2A''(X^2B_1)$						
R(S–M)	0.935			1.879[a] ($/1^4A''$)	4.0	$H_2(X^1\Sigma_g^+) + S^+(^2D)$
ΔE	0.0			3.50[b]	4.82	4.84
$1^2A'(A^2A_1)$						
R(S–M)	0.610	1.194	1.481	1.802[a] ($/1^4A''$)	4.0	$H_2(X^1\Sigma_g^+) + S^+(^2D)$
ΔE	2.38	4.06	3.20	3.59[c]	4.85	4.84
$1^4A''$						
R(S-M)					4.0	$H_2(X^1\Sigma_g^+) + S^+(^4S)$
ΔE					2.92	2.92

The CASSCF MECPs are actually not along the CASPT2 PECs; see footnotes a–c

[a] The R(S–M) values in the CASSCF MECP geometries

[b] The CASPT2 relative energy (to $X^1B_{1)}$ of the $1^2A''$ state at the $1^2A''/1^4A''$ MECP

[c] The CASPT2 relative energy (to $X^1B_{1)}$ of the $1^2A'$ state at the $1^2A'/1^4A''$ MECP

As shown in Fig. 2, the $1^4A''$ state is essentially a repulsive state (there may be a shallow minimum at a R(S–M) value of around 3.0 Å) while the $1^2A''$ state is a bound state. Along the $1^2A'$ PEC there are transition state (TS) at a R(S–M) value of 1.19 Å and intermediate (IM, a local minimum) at a R(S–M) value of 1.48 Å. The CASPT2 full geometry optimization calculations produced a C_s geometry for TS ($1^2A'$) and a C_{2v} geometry for IM ($1^2A'$) (the two optimized geometries are given in Table 1). At the CASPT2 TS ($1^2A'$) geometry the CASPT2 energy gap between the $1^2A'$ and $2^2A'$ states was calculated to be 0.48 eV. The CASPT2 calculations predict that TS ($1^2A'$) and IM ($1^2A'$) are 4.06 and 3.20 eV above the X^2B_1 reactant and 1.68 and 0.82 eV above the A^2A_1 reactant, respectively. In the CASSCF wave functions of the TS ($1^2A'$) and IM ($1^2A'$), we found the same dominant configuration $[\ldots(4a')^2(1a'')^2(5a')^2(6a')^2(7a')^1(2a'')^2]$ with coefficients of 0.959 and 0.965, respectively. The CASPT2 relative energies (to X^2B_1) of the TS ($1^2A'$) and IM ($1^2A'$) are also given in Table 2.

3.2 CASPT2 H-loss dissociation potential energy curves for the low-lying states

We calculated H-loss dissociation PECs for the $1^2A''(X^2B_1)$ and $1^2A'(A^2A_1)$ states of the H_2S^+ ion. We also calculated the H-loss dissociation PEC of the $1^4A''(1^4A_2)$ state. As we will see below, this state correlates with the first limit of the H-loss dissociation and its PEC crosses the $1^2A'$ PEC.

The H-loss dissociation PECs for the three states were calculated at the CASPT2 level. At a set of fixed R(S–H_2) (Fig. 1) values ranging from the R(S–H_2) values in the CASPT2 optimized geometries of the respective states (from R(S–H_2) = 1.70 Å for $1^4A''$) to 5.0 Å, the CASPT2 partial geometry optimization calculations were performed for the three states. The H-loss dissociation PECs for the $1^2A''$, $1^2A'$, and $1^4A''$ states were drawn in Fig. 3 on the basis of the CASPT2 energies at the three sets of partially optimized geometries. The H_2S^+ systems in the three states at the R(S–H_2) value of 5.0 Å will be called as H-loss dissociation asymptotic products of the respective states in the present article.

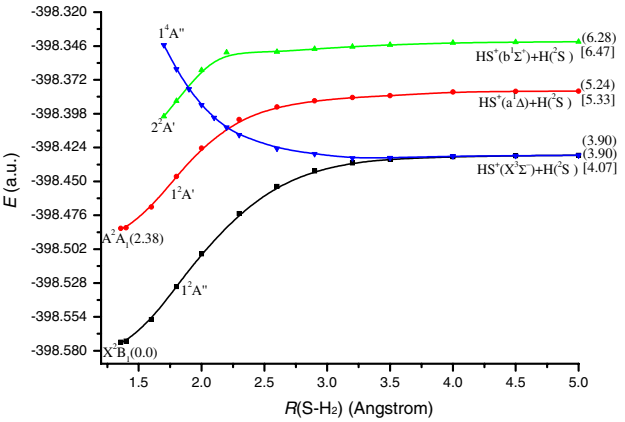

Fig. 3 CASPT2 PECs for H-loss dissociation from the $1^2A''$ (X^2B_1), $1^2A'$ (A^2A_1), and $1^4A''$ states of the H_2S^+ ion (the $2^2A'$ curve is also given). The values in parentheses are the CASPT2 energies (relative to X^2B_1, in eV) of the reactants and asymptotic products and the *values* in square brackets are the CASPT2 energies (energy sums) (relative to X^2B_1, in eV) of the dissociation products. The CASPT2 PEC for the $2^2A'$ state is also CASPT2 PECs

Very small charge values (less than 0.001e) at the departing H atom (H_2) in the asymptotic products indicate that the dissociation products from the three states are the neutral H atom plus the HS^+ ion in different electronic

states. The CASPT2 geometry optimization calculations (see Sect. 2) for the $X^3\Sigma^-$, $a^1\Delta$, and $b^1\Sigma^+$ states of the HS^+ ion were performed. The CASPT2 relative energy values of 1.26 and 2.40 eV for the $a^1\Delta$ and $b^1\Sigma^+$ states (to $X^3\Sigma^-$) are in good agreement with the experimental values of 1.2800 and 2.3899 eV [30], respectively. The bond length values in the CASPT2 geometries of the $X^3\Sigma^-$, $a^1\Delta$, and $b^1\Sigma^+$ states are 1.374, 1.365, and 1.363 Å, respectively. The CASPT2 energy sums for $HS^+(X^3\Sigma^-) + H(^2S)$, $HS^+(a^1\Delta) + H(^2S)$, and $HS^+(b^1\Sigma^+) + H(^2S)$ are 4.07, 5.33, and 6.47 eV above the X^2B_1 reactant, respectively [in the evaluation an energy value of 0.5 a.u. was taken for $H(^2S)$]. The three product groups correspond to the first, second, and third limits of the H-loss dissociation, respectively.

The S–H_1 bond length values (1.362–1.366 Å) in the three asymptotic products are very close to the CASPT2 S–H bond length values (1.363–1.374 Å) for the $X^3\Sigma^-$, $a^1\Delta$, and $b^1\Sigma^+$ states of the HS^+ ion. The CASPT2 energy values for the $1^2A''$ and $1^4A''$ asymptotic products are close to the CASPT2 energy sum of $HS^+(X^3\Sigma^-) + H(^2S)$ (the deviations being 0.17 eV), which confirms that the H-loss dissociation products from the $1^2A''(X^2B_1)$ and $1^4A''$ states of the H_2S^+ ion are $[HS^+(X^3\Sigma^-) + H(^2S)]$ (the first limit for H-loss dissociation). The CASPT2 energy value for the $1^2A'$ asymptotic product is close to the CASPT2 energy sum for $HS^+(a^1\Delta) + H(^2S)$ (the deviation being 0.09 eV), which confirms that the H-loss dissociation products from the $1^2A'$ (A^2A_1) state of the H_2S^+ ion are $[HS^+(a^1\Delta) + H(^2S)]$ (the second limit for H-loss dissociation). The CASPT2 relative energies (to X^2B_1) of the reactants, asymptotic products, and products for the H-loss dissociation from the $1^2A''$ (X^2B_1), $1^2A'$ (A^2A_1), and $1^4A''$ states are given in Table 3.

Table 3 The critical points [reactants, asymptotic products (AsP), and products] along the CASPT2 H-loss dissociation PECs of the $1^2A''$ (X^2B_1), $1^2A'$ (A^2A_1), and $1^4A''$ (1^4A_2) states of the H_2S^+ ion: locations [R(S–H_2) values in Å] and relative energies (ΔE in eV, to X^1B_1)

State	Reactant	AsP	Products
$1^2A''$ (X^2B_1)			
R(S–H_2)	1.357	5.0	$HS^+(X^3\Sigma^-) + H(^2S)$
ΔE	0.0	3.90	4.07
$1^2A'$ (A^2A_1)			
R(S–H_2)	1.356	5.0	$HS^+(a^1\Delta) + H(^2S)$
ΔE	2.38	5.24	5.33
$1^4A''$			
R(S–H_2)		5.0	$HS^+(X^3\Sigma^-) + H(^2S)$
ΔE		3.90	4.07

3.3 Discussion on photodissociation of the *A* state

We will examine the two previously suggested mechanisms (I and II) for the S-loss dissociation from the *A* state of the H_2S^+ ion in Sect. 3.3.1. We will consider the H-loss dissociation from the *A* state in Sect. 3.3.2. We will present our conclusions on photodissociation of the *A* state in Sect. 3.3.3.

3.3.1 Discussion on photodissociation of the A state to the S^+ ion

Before discussion we should perform more calculations (the MECP and Renner–Teller curve calculations).

In the figure (Fig. 2) of the S-loss dissociation PECs, the $1^4A''$ PEC crosses the $1^2A''$ and $1^2A'$ PECs, which imply the crossings between the $1^2A''$ and $1^4A''$ PESs and between the $1^2A'$ and $1^4A''$ PESs. We performed the CASSCF MECP calculations for the $1^2A''/1^4A''$ and $1^2A'/1^4A''$ state pairs. In Table 4 we report the geometries and spin-orbit couplings at the $1^2A''/1^4A''$ and $1^2A'/1^4A''$ MECPs calculated at the CASSCF level, together with the CASPT2 energies (relative to X^2B_1) for the states in pairs calculated at the CASSCF MECPs. The large spin-orbit coupling values at the $1^2A''/1^4A''$ and $1^2A'/1^4A''$ MECPs (467 and 463 cm^{-1}, respectively) imply strong interactions. At the two CASSCF MECPs, the CASPT2 energy differences between the doublet and quartet states in pairs are smaller than 0.1 eV (within the error of the CASPT2 energy calculations: 0.3 eV). The CASPT2 relative energy (to X^2B_1) of the $1^2A''$ state at the $1^2A''/1^4A''$ MECP is 3.50 eV and the CASPT2 relative energy (to X^2B_1) of the $1^2A'$ state at the $1^2A'/1^4A''$ MECP is 3.59 eV. These two important energy values are listed in proper rows of Table 2, together with the R(S–M) values (1.879 and 1.802 Å, respectively) in the $1^2A''/1^4A''$ and $1^2A'/1^4A''$ (CASSCF) MECP geometries, though the MECPs are not along the PECs.

We calculated the $E(\theta = \angle HSH)$ PECs for the X^2B_1 and A^2A_1 states of the H_2S^+ ion at the CASPT2 level. At a set of fixed θ values ranging from 80.0° to 180.0° we carried out CASPT2 partial geometry optimization calculations for the X^2B_1 and A^2A_1 states, and the $E(\theta)$ PECs obtained in these calculations are given in Fig. 4. At the θ value of 180.0° the X^2B_1 and A^2A_1 states should be the two components of the $^2\Pi_u$ state, but the CASPT2 energy values for the two component states are slightly different (the discrepancy of 0.05 eV being within the error of the CASPT2 calculations). In our CASPT2 calculations, the barriers at the linearity for the X^2B_1 and A^2A_1 states are predicted to be 2.91 and 0.58 eV, which are in good agreement with the experimental values of 2.877 and 0.572 eV [31–33], respectively.

Table 4 The $1^2A''/1^4A''$ and $1^2A'/1^4A''$ MECPs in the S-loss dissociation reactions of the H_2S^+ ion: the CASSCF MECP geometries and CASSCF spin-orbit couplings (in cm^{-1}) at the MECPs and the CASPT2 energies ($\Delta E/\Delta E$ in eV, relative to X^2B_1) for the states in pairs calculated at the CASSCF MECPs (bond lengths are in Å and bond angles in degrees)

State/state	CASSCF MECP geometry			CASSCF spin–orbit coupling	CASPT2 $\Delta E/\Delta E$[a]
	R(S–M)	$R(H_1–H_2)$	$\angle SMH_2$		
$1^2A''/1^4A''$	1.879	0.814	90.2	467.5	3.50/3.46
$1^2A'/1^4A''$	1.802	0.814	90.0	463.2	3.59/3.69

At the CASSCF MECPs, the CASSCF energy differences between the doublet and quartet states in pairs are smaller than 5.4×10^{-5} a. u

[a] At the CASSCF MECPs, the CASPT2 energy differences between the doublet and quartet states in pairs are smaller than 0.10 eV (within the error of the CASPT2 energy calculations: 0.3 eV)

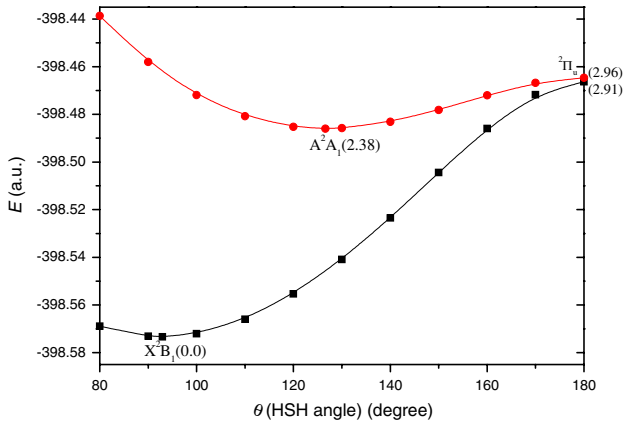

Fig. 4 The CASPT2 $E(\theta)$ PECs for the X^2B_1 and A^2A_1 states of the H_2S^+ ion in the C_{2v} symmetry (θ denotes the HSH bond angle). The *values* in parentheses are the CASPT2 relative energies (to X^2B_1, in eV)

On the basis of our CASPT2 PEC and CASSCF MECP calculation results we now examine the two previously proposed mechanisms (I and II) for dissociation of the A state to the S^+ ion. In mechanism I of Hirsch et al. [2], the A^2A_1 state was proposed to nonadiabatically transit to the B^2B_2 state via strong vibronic coupling. In the figures (for example, see Ref. [3]) of the $E(\theta)$ PECs for the C_{2v} states of the H_2S^+ ion, there is a crossing between the A^2A_1 and B^2B_2 PECs. We understand that the "strong vibronic coupling" mentioned by Hirsch et al. [2] referred to this PEC crossing. However, in the C_s symmetry the $1^2A'$ and $2^2A'$ PECs (Fig. 2) do not cross. Instead of saying "transition of A^2A_1 to B^2B_2 via strong vibronic coupling", we say that in the S-loss dissociation process the ionic system in the $1^2A'$ state should override the transition state ($1^2A'$) (Fig. 2) which has a C_s geometry (Table 1). We therefore suggest a process (denoted as process I, based on mechanism I [2]) for photodissociation of the A state to the S^+ ion as follows (the CASPT2 relative energy values to X^2B_1 are given in parentheses): A^2A_1 ($1^2A'$) (2.38 eV) → transition state ($1^2A'$) (4.06 eV) → intermediate ($1^2A'$) (3.20 eV) → the $1^2A'/1^4A''$ MECP (3.59 eV) → $S^+(^4S) + H_2(X^1\Sigma_g^+)$ (2.92 eV). The last two steps in process I describe the predissociation of $1^2A'$ by $1^4A''$ (the spin–orbit coupling value at the $1^2A'/1^4A''$ MECP is large). Along process I, the transition state ($1^2A'$) is the critical point having the highest energy of 4.06 eV (relative to X^2B_1). Following mechanism II of Dixon et al. [10], we give another process (denoted as process II) for photodissociation of the A state to the S^+ ion as follows (the CASPT2 relative energy values to X^2B_1 are given in parentheses): A^2A_1 ($1^2A'$) (2.38 eV) → barrier at the linearity (2.96 eV) → X^2B_1 ($1^2A''$) (0.0 eV) → the $1^2A''/1^4A''$ MECP (3.50 eV) → $S^+(^4S) + H_2(X^1\Sigma_g^+)$ (2.92 eV). The first two steps describe a nonadiabatical transition of A^2A_1 to X^2B_1 via Renner–Teller coupling and the last two steps describe the predissociation of X^2B_1 by $1^4A''$ (the spin-orbit coupling value at the $1^2A''/1^4A''$ MECP is large). Along process II, the $1^2A''/1^4A''$ MECP is the critical point having the highest energy of 3.50 eV (relative to X^2B_1). Dixon et al. [10] knew that the barrier at the linearity for A^2A_1 be low, but they might not know that the predissociation of $1^2A''$ (X^2B_1) by $1^4A''$ needs more energy.

The CASPT2 energy (3.50 eV, relative to X^2B_1) at the highest-energy point along process II is lower than the CASPT2 energy (4.06 eV, relative to X^2B_1) at the highest-energy point along process I. Therefore we conclude that, for photodissociation of the A state of the H_2S^+ ion to the S^+ ion, process II represents the most probable mechanism. We denote the CASPT2 energy value (relative to X^2B_1) at the highest-energy point along a process as the E_{ae} (a quantity similar to "appearance energy") value for that process. Then the E_{ae} values for process I and process II are 4.06 and 3.50 eV, respectively.

3.3.2 *Discussion on photodissociation of the A state to the HS^+ ion*

In the figure (Fig. 3) of the H-loss dissociation PECs the $1^4A''$ PEC crosses the $1^2A'$ PEC, which implies the crossing between the $1^2A'$ and $1^4A''$ PESs and possible predissociation of the $1^2A'$ state by the $1^4A''$ state leading to the first limit for H-loss dissociation [$HS^+(X^3\Sigma^-) + H(^2S)$].

We performed the CASSCF MECP calculations for the $1^2A'/1^4A''$ state pair, with the CASPT2 partially optimized geometry of the $1^2A'$ state at R(S–H$_2$) = 2.21 Å (along the $1^2A'$ H-loss dissociation PEC) as a starting geometry. We will denote this MECP as the "$1^2A'/1^4A''$ MECP (to HS^+)" since in the photodissociation process of the A state to the S^+ ion there is already a "$1^2A'/1^4A''$ MECP" (see Sect. 3.3.1). However, the CASSCF calculations for searching the $1^2A'/1^4A''$ MECP (to HS^+) were not successful (the calculations produced a strange geometry for the $1^2A'/1^4A''$ MECP (to HS^+) which is very much different from the starting geometry).

Though the geometry of the $1^2A'/1^4A''$ MECP (to HS^+) was not successfully located, we can still suggest a process (denoted as process III) for photodissociation of the A state to the HS^+ ion as follows (the CASPT2 relative energy values to X^2B_1 are given in parentheses): A^2A_1 ($1^2A'$) (2.38 eV) → the $1^2A'/1^4A''$ MECP (to HS^+) (? eV) → $HS^+(X^3\Sigma^-)$ + H(^{2}S) (4.07 eV). Process III just describes the predissociation of $1^2A'$ by $1^4A''$ [we assume that the spin-orbit coupling value at the $1^2A'/1^4A''$ MECP (to HS^+) is not too small]. We can not give the E_{ae} value for process III since the energy at the $1^2A'/1^4A''$ MECP (to HS^+) is not known. However, the E_{ae} value for process III should be larger than (or equal to) the CASPT2 energy (relative to X^2B_1) of the product, that is, $E_{ae} \geq 4.07$ eV.

3.3.3 *Conclusions on photodissociation of the A state*

The E_{ae} value (3.50 eV) for process II (S-loss, to S^+) is smaller than the E_{ae} value (4.06 eV) for process I (S-loss, to S^+) and the E_{ae} value (≥4.07 eV) for process III (H-loss, to HS^+). We can conclude that (1) photodissociation from the A state of the H_2S^+ ion mainly leads to the product S^+ ion and (2) that process II represents the most probable mechanism for photodissociation of the A state of the H_2S^+ ion to the S^+ ion. Conclusion (1) supports the conclusion of Eland [8] and Prest et al. [12] based on their experiments. Conclusion (2) supports mechanism II suggested by Dixon et al. [10] though they might not know that the predissociation of $1^2A''$ (X^2B_1) by $1^4A''$ needs more energy.

3.4 Preliminary discussion on the photodissociation of the X and B states

As shown in Fig. 3, the X^2B_1 ($1^2A''$) state of the H_2S^+ ion can directly (adiabatically) dissociate to the first limit [$HS^+(X^3\Sigma^-)$ + H(^{2}S)] of the H-loss dissociation, and the dissociation energy is evaluated to be 4.07 eV at the CASPT2 level. As shown in Fig. 2, the X^2B_1 ($1^2A''$) state of the H_2S^+ ion does not correlate with the first limit [$H_2(X^1\Sigma_g^+)$ + $S^+(^4S)$] of the S-loss dissociation, but the crossing between the $1^2A''$ and $1^4A''$ PECs implies a possible predissociation of the $1^2A''$ (X^2B_1) state by the $1^4A''$ state leading to the first limit [$H_2(X^1\Sigma_g^+)$ + $S^+(^4S)$]. As we mentioned in Sect. 3.3.1, the spin-orbit coupling value at the $1^2A''/1^4A''$ MECP (to $S^{+)}$ is very large and the CASPT2 energy (relative to X^2B_1) of the $1^2A''$ state at the $1^2A''/1^4A''$ MECP is 3.50 eV (Table 4). Since this energy value is smaller than the CASPT2 dissociation energy of 4.07 eV to [$HS^+(X^3\Sigma^-)$ + H(^{2}S)], we conclude that dissociation from the X state of the H_2S^+ ion will lead to the product S^+ ion. This is a purely theoretical argument and there is no available experimental information.

The CASPT2 H-loss dissociation PEC calculations indicate that the $2^2A'$ state of the H_2S^+ ion correlates with the third limit of [$HS^+(b^1\Sigma^+)$ + H(^{2}S)] for the H-loss dissociation, which is 6.47 eV above the X^2B_1 reactant. The crossing between the $2^2A'$ and $1^4A''$ PECs (Fig. 3) implies a possible predissociation of the $2^2A'$ state by the $1^4A''$ state leading to the first limit [$HS^+(X^3\Sigma^-)$ + H(^{2}S)] of the H-loss dissociation. The CASSCF MECP calculations for the $2^2A'/1^4A''$ state pair were successful. The CASSCF spin-orbit coupling value (33 cm^{-1}) at the $2^2A'/1^4A''$ MECP is not too small and the CASPT2 relative energy (to X^2B_1) of the $2^2A'$ state at the $2^2A'/1^4A''$ MECP is 5.23 eV. The S-loss dissociation PEC of the $2^2A'$ state was not calculated.

4 Concluding remarks

The PECs given in Figs. 2 and 3 are actually the minimum-energy paths for the adiabatic S- and H-loss dissociation from the different states of the H_2S^+ ion. These PECs were drawn on the basis of many sets of CASPT2 partial geometry optimization calculations, and the CASPT2 geometry optimization technique (using numerical gradients) was developed just in these years. Such PECs are basically important for further studies on photodissociation of molecular ions. The PEC crossings in the two figures suggest us to perform CASSCF MECP calculations for the relevant states in pairs. We understand that the geometry, as the result of the MECP calculations using the MOLCAS programs for two states in pair, is at the minimum-energy point in the intersection seam (it is a two-dimensional surface in the case of H_2S^+) between the two potential energy surfaces. The MECP calculations can be carried out only at the CASSCF level, but the searching for the MECP geometry is automatic. The two techniques (CASPT2 geometry optimization and CASSCF MECP searching) help us to carry out more effective (less computing efforts and more accurate) study on photodissociation of the H_2S^+ ion than previous theoretical researchers.

On the basis of our calculation results we have considered the following three processes for the photodissociation of the A state of the H_2S^+ ion:

1. Process I (to the S^+ ion): $A^2A_1(1^2A') \rightarrow$ transition state $(1^2A') \rightarrow$ intermediate $(1^2A') \rightarrow 1^2A'/1^4A''$ MECP $\rightarrow S^+(^4S) + H_2$, ($E_{ae}$ = 4.06 eV);
2. Process II (to the S^+ ion): $A^2A_1(1^2A') \rightarrow$ barrier at linearity $\rightarrow X^2B_1(1^2A'') \rightarrow 1^2A''/1^4A''$ MECP $\rightarrow S^+(^4S) + H_2$, ($E_{ae}$ = 3.50 eV), and
3. Process III (to the HS^+ ion): A^2A_1 $(1^2A') \rightarrow 1^2A'/1^4A''$ MECP (to HS^+) $\rightarrow HS^+(X^3\Sigma^-) + H$, ($E_{ae} \geq$ 4.07 eV).

By comparing the CASPT2 E_{ae} values for the three processes, we conclude that the A state of the H_2S^+ ion mainly dissociates to the S^+ ion via process II (E_{ae} = 3.50 eV). We also present a preliminary discussion on dissociation from the X and B states of the H_2S^+ ion.

Acknowledgment We appreciate the financial support of this work that was provided by National Natural Science Foundation of China through Contract No. 20773161.

References

1. Hirst DM (2003) J Chem Phys 118:9175–9184. doi:10.1063/1.1568080
2. Hirsch G, Bruna PJ (1980) Int J Mass Spectrom Ion Phys 36:37–46. doi:10.1016/0020-7381(80)80005-2
3. Li WZ, Huang MB (2005) Chem Phys 315:133–141. doi:10.1016/j.chemphys.2005.04.005
4. Webb AD, Dixon RN, Ashfold MNR (2007) J Chem Phys 127:224307. doi:10.1063/1.2800559
5. Webb AD, Kawanaka N, Dixon RN, Ashfold MNR (2007) J Chem Phys 127:224308. doi:10.1063/1.2800565
6. Dibeler VH, Rosenstock HM (1963) J Chem Phys 39:3106–3111. doi:10.1063/1.1734150
7. Dibeler VH, Liston SK (1968) J Chem Phys 49:482–485. doi:10.1063/1.1670100
8. Eland JHD (1979) Int J Mass Spectrom Ion Phys 31:161–173. doi:10.1016/0020-7381(79)80115-1
9. Möhlmann GR, Deheer FJ (1975) Chem Phys Lett 15:353–356. doi:10.1016/0009-2614(75)80254-5
10. Dixon RN, Duxbury G, Horani M, Rostas J (1971) Mol Phys 22:977–992. doi:10.1080/00268977100103311
11. Edwards CP, Maclean CS, Sarre PJ (1982) Chem Phys Lett 87:11–13. doi:10.1016/0009-2614(82)83542-2
12. Prest HF, Tzeng WB, Brom JM Jr, Ng CY (1983) Int J Mass Spectrom Ion Phys 50:315–329. doi:10.1016/0020-7381(83)87008-9
13. Jarrold MF, Illies AJ, Bowers MT (1982) Chem Phys 65:19–28. doi:10.1016/0301-0104(82)85052-0
14. Ibuki T (1984) J Chem Phys 81:2915–2918. doi:10.1063/1.448038
15. Tokue I, Yamasaki K, Nanbu S (2003) J Chem Phys 119:5882–5888. doi:10.1063/1.1602064
16. Carney TE, Baer T (1981) J Chem Phys 75:4422–4429. doi:10.1063/1.442607
17. Fiquet-Fayard F, Guyon PM (1966) Mol Phys 11:17–30. doi:10.1080/00268976600100811
18. Feng RF, Cooper G, Brion CE (1999) Chem Phys 249:223–236. doi:10.1016/S0301-0104(99)00232-3
19. Hochlaf M, Weitzel KM (2004) J Chem Phys 120:6944–6956. doi:10.1063/1.1669386
20. Tokue I, Yamasaki K, Nanbu S (2003) J Chem Phys 119:5874–5881. doi:10.1063/1.1602063
21. Roos BO (1987) Adv Chem Phys 69:399–445. doi:10.1002/9780470142943.ch7
22. Andersson K, Roos BO (1993) Int J Quantum Chem 45:591–607. doi:10.1002/qua.560450610
23. Andersson K, Malmqvist P, Roos BO (1995) In: Yarkony DR (ed) Modern electronic structure theory. World Scientific, Singapore, vol 1, p 55
24. Chang HB, Chen BZ, Huang MB (2008) J Phys Chem A 112:1688–1693. doi:10.1021/jp710633s
25. Andersson K et al (2005) MOLCAS (version 6.2). University of Lund, Sweden
26. Almlof J, Taylor PR (1987) J Chem Phys 86:4070–4077. doi:10.1063/1.451917
27. Widmark PO, Malmqvist PA, Roos BO (1990) Theor Chim Acta 77:291–306. doi:10.1007/BF01120130
28. Widmark PO, Persson BJ, Roos BO (1991) Theor Chim Acta 79:419–432. doi:10.1007/BF01112569
29. Huber KP, Herzberg G (1979) Molecular spectra and molecular structure IV. Constants of diatomic molecules. Van Nostrand Reinhold Co., New York
30. Dunlavey SJ, Dyke JM, Fayad NK, Jonathan N, Morris A (1979) Mol Phys 38:729. doi:10.1080/00268977900102001
31. Turner DW, Baker C, Baker AD, Brundle CR (1970) Molecular photoelectron spectroscopy. Wiley, London
32. Duxbury G, Horani M, Rostas J (1972) Proc R Soc Lond A 331:109
33. Duxbury G, Jungen C, Rostas J (1983) Mol Phys 48:719. doi:10.1080/00268978300100541
34. Potts AW, Price WC (1972) Proc R Soc A 326:181–197. doi:10.1098/rspa.1972.0004